



UNIVERSITÀ DI PARMA

ARCHIVIO DELLA RICERCA

University of Parma Research Repository

Pressure Effects on Water Dynamics by Time-Resolved Optical Kerr Effect

This is the peer reviewed version of the following article:

Original

Pressure Effects on Water Dynamics by Time-Resolved Optical Kerr Effect / Taschin, Andrea; Bartolini, Paolo; Fanetti, Samuele; Lapini, Andrea; Citroni, Margherita; Righini, Roberto; Bini, Roberto; Torre, Renato. - In: THE JOURNAL OF PHYSICAL CHEMISTRY LETTERS. - ISSN 1948-7185. - 11:8(2020), pp. 3063-3068. [10.1021/acs.jpcllett.0c00363]

Availability:

This version is available at: 11381/2891150 since: 2024-12-17T10:55:29Z

Publisher:

American Chemical Society

Published

DOI:10.1021/acs.jpcllett.0c00363

Terms of use:

Anyone can freely access the full text of works made available as "Open Access". Works made available

Publisher copyright

note finali coverpage

(Article begins on next page)

02 May 2026

This document is confidential and is proprietary to the American Chemical Society and its authors. Do not copy or disclose without written permission. If you have received this item in error, notify the sender and delete all copies.

Pressure Effects on the Water Dynamics by Time-Resolved Optical Kerr Effect

Journal:	<i>The Journal of Physical Chemistry Letters</i>
Manuscript ID	jz-2020-00363s.R1
Manuscript Type:	Letter
Date Submitted by the Author:	10-Mar-2020
Complete List of Authors:	Taschin, Andrea; Universita degli Studi di Firenze Laboratorio Europeo di Spettroscopie Non Lineari, Universita di Firenze; ENEA National Agency for New Technologies Energy and Economic Sustainable Development Bartolini, Paolo; Universita degli Studi di Firenze Laboratorio Europeo di Spettroscopie Non Lineari, Fanetti, Samuele; ICCOM CNR; Universita degli Studi di Firenze Laboratorio Europeo di Spettroscopie Non Lineari Lapini, Andrea; INRIM; Universita degli Studi di Firenze Laboratorio Europeo di Spettroscopie Non Lineari Citroni, Margherita; Universita degli Studi di Firenze Laboratorio Europeo di Spettroscopie Non Lineari Righini, Roberto; Universita degli Studi di Firenze Laboratorio Europeo di Spettroscopie Non Lineari; Universita degli Studi di Firenze Dipartimento di Chimica Ugo Schiff Bini, Roberto; Universita degli Studi di Firenze Dipartimento di Chimica Ugo Schiff; Universita degli Studi di Firenze Laboratorio Europeo di Spettroscopie Non Lineari; ICCOM CNR Firenze Torre, Renato; Universita degli Studi di Firenze Laboratorio Europeo di Spettroscopie Non Lineari, European lab for Non-Linear Spectroscopy; Universita degli Studi di Firenze Dipartimento di Fisica e Astronomia

SCHOLARONE™
Manuscripts

Pressure Effects on the Water Dynamics by Time-Resolved Optical Kerr Effect

Andrea Taschin,^{*,†} Paolo Bartolini,[†] Samuele Fanetti,^{†,‡} Andrea Lapini,^{†,¶}

Margherita Citroni,[†] Roberto Righini,^{†,§} Roberto Bini,^{†,‡,§} and Renato Torre^{†,||}

[†]*European Lab. for Non-Linear Spectroscopy (LENS), Univ. di Firenze, via N. Carrara 1,
I-50019 Sesto Fiorentino, Firenze, Italy.*

[‡]*ICCOM, Istituto di Chimica dei Composti OrganoMetallici, Via Madonna del Piano 10,
I-50019 Sesto Fiorentino, Firenze, Italy.*

[¶]*INRIM, Istituto Nazionale di Ricerca Metrologica, Strada delle Cacce 91, I-10135 Torino,
Italy.*

[§]*Dip. di Chimica "Ugo Schiff", Univ. di Firenze, via Della Lastruccia 13, I-50019 Sesto
Fiorentino, Firenze, Italy.*

^{||}*Dip. di Fisica e Astronomia, Univ. di Firenze, via G. Sansone 1, I-50019 Sesto
Fiorentino, Firenze, Italy.*

E-mail: taschin@lens.unifi.it

Abstract

Despite being water the most common and most widely studied substance in the world, it still presents unknown aspects. In particular, water shows several thermodynamic and dynamical anomalies in the liquid and supercooled metastable phases, whose nature is still hotly debated. Here we report measurements by Optical Kerr Effect on water as a function of pressure along two isotherms, at 273 K from 0.1 to 750 MPa and at 297 K from 0.1 MPa to 1350 MPa, reaching the supercooled metastable

1
2
3 phase. The structural relaxation and the low frequency vibrational dynamics of water
4 show a peculiar pressure dependence, similar to that of other dynamical properties.
5
6 The data analysis suggests the presence in the water phase-diagram of a crossover area
7 that divides two regions characterized by different dynamic regimes, which appear to
8
9 be related to two liquid forms, one dominated by the high density water and the other
10
11 by the low density water.
12
13
14

15
16 Water shows a series of unexpected physical properties both in liquid and metastable
17 phases¹; despite the different physical models and thermodynamic interpretations proposed²,
18 the origin of these anomalies is still unclear and subject of an intense debate³⁻⁷. It is widely
19 accepted that water anomalies are connected with the local structural arrangement, char-
20 acterized by a temperature and pressure dependent degree of order that affect the dynamic
21 properties^{7,8} of the liquid. Among the several theoretical models proposed², the second
22 critical point (SCP) hypothesis⁹ is the more accredited and debated. This model hypothes-
23 izes the existence of a first order phase transition between the low-density (LDW) and the
24 high-density (HDW) water forms; the low-density phase is characterized by tetrahedral inter-
25 molecular coordination, while the high-density one shows more closely packed structures with
26 distorted hydrogen bond network. The phase transition would exist only in the deep super-
27 cooled phase and would terminate in a liquid-liquid critical point (LLPC). The predictions of
28 the SCP model are supported by a series of computational results, and are compatible with
29 many experimental results^{2,10,11}; nevertheless, the crystallization process limits the experi-
30 mental investigations in a phase diagram region where the observed anomalous properties
31 cannot be exclusively attributed to the LLCP existence.
32
33
34
35
36
37
38
39
40
41
42
43
44
45
46

47
48 In this scenario, continuous efforts aim to realize new experimental investigations to un-
49 ravel the water mystery, leading liquid water beyond the metastable phase limit^{12,13} and/or
50 measuring new unexplored physical observables^{14,15}. The high pressure states of liquid wa-
51 ter certainly represent a unexplored region of the phase diagram that can give new valuable
52 information. The pressure dependence of different dynamical properties of water has been
53
54
55
56
57
58
59
60

1
2
3 the subject of several investigations^{16–25}. All these experimental studies evidenced the pres-
4 sure variation of several dynamical parameters along the isotherms that was attributed to
5 changes of the local structural arrangement. The nature of these anomalies remains not
6 fully explained but it is accepted that they are related to the pressure induced collapse of
7 the second molecular solvation shell into the first one, correlated with the conversion from
8 LDW to HDW water form; nevertheless, the connection between these phenomena and the
9 LLCPC hypothesis has not yet been clarified.

10
11 Recently, the thermodynamic and dynamical anomalies of water were successfully ex-
12 plained by the two-state model^{3,10,25–31}, which describes water as an athermal nonideal
13 solution of two states, or structures, that quickly interconvert. The mixing ratio of the
14 two species is a function of temperature and pressure. At low temperatures the system
15 undergoes a phase separation in two different liquids, which terminates at a liquid-liquid
16 critical point. The success of the two-state model reinforces the description of pure water
17 as a bimodal distribution of local structures against the continuous model, in which all local
18 structures should exist with equal probability. In the two-state picture, the coexistence of
19 the LDW and HDW forms should not be seen as resulting from static inhomogeneity of the
20 liquid, but rather as due to the equilibrium between rapidly (on the molecular time scale)
21 interconverting local structures. A direct measurement of structural dynamics can provide
22 valuable information on water modeling, in particular on the diatribe between bimodal and
23 continuous structuring.

24
25 Here, we report on the investigation of water dynamics as a function of pressure at 273 *K*
26 and at 297 *K*. We used a non-linear time-resolved spectroscopic technique, the Heterodyne
27 Detected Optical Kerr Effect (HD-OKE) experiment³². In most simple molecular liquids, the
28 relaxation of the OKE signal is interpreted in terms of single molecule orientational diffusion;
29 on the contrary, the anisotropy of the molecular polarizability of water is so low that the
30 optically induced polarization is dominated by intermolecular contributions. Thus, the long
31 time decay of the measured signal of liquid water is associated with the rearrangement of

1
2
3 hydrogen-bonded extensive structures, i.e. with the first step of the structural relaxation.
4
5 In parallel, the short time part of the signal accounts for the intermolecular vibrational
6
7 dynamics, which provides additional information on the collective behavior of the liquid.
8
9 The technique allows measuring the structural relaxation processes and the low frequency
10
11 vibrational dynamics of water with unprecedented data quality^{14,32,33}. This is the first time
12
13 that HD-OKE is used to study compressed water. The only attempt, so far reported in
14
15 the literature, to measure OKE on a pressurized liquid, concerned carbon disulfide³⁴, whose
16
17 nonlinear signal is orders of magnitude stronger than that of water. Moreover HD-OKE
18
19 measures the water collective dynamics that remains poorly explored at high pressure due
20
21 to the intrinsic experimental difficulties; only viscosity²⁵ and water sound velocity have been
22
23 investigated so far^{35,36}. For the analysis of the experimental results we adopted the two
24
25 state model, following the approach proposed by Singh et al.²⁵ for the interpretation of the
26
27 pressure dependence of other dynamic observables of water.
28

29
30 In the HD-OKE experiment, a polarized short laser pulse (the pump) induces a transi-
31
32 ent optical birefringence in the sample, corresponding to the coherence of vibrational and
33
34 rotational/librational states induced via stimulated Raman coupling³⁷. The time evolution
35
36 of the induced birefringence, due to the relaxation of those coherent states, is monitored by
37
38 a second delayed laser pulse (the probe). The experiment measures the third order response
39
40 function, which is directly connected to the time derivative of the correlation function of
41
42 the first order anisotropic susceptibility. The measured signal contains information on the
43
44 diffusion/relaxation processes and on the low-frequency vibrational dynamics of the sample.
45
46 The laser pulses, centered at the wavelength of 800 *nm*, have a duration of 15 *fs* (more ex-
47
48 perimental details can be found in Supporting Information (SI), section S.1.2 and in ref.³²).
49
50 Recent experimental improvements provide access to a very large time/frequency window,
51
52 covering the whole inter-molecular water dynamics³². Nevertheless, the extraction of the
53
54 water response function from the intrinsically very weak HD-OKE signal is far from being a
55
56 trivial procedure, and relies on the knowledge of the appropriate instrumental function and
57
58
59
60

1
2
3 on the consequent correct deconvolution of the HD-OKE signal (see SI, section S.1.4 for more
4 details). We performed the high pressure experiments on bi-distilled water samples held in
5 a diamond anvil cell (DAC) with a gasket having initial thickness of $\sim 250\mu m$ and initial
6 diameter of $\sim 500\mu m$ (see SI). Temperature has been controlled by means of a nitrogen
7 continuous-flow cryostat equipped with a thermocouple fixed on the sample cell (accuracy
8 of $\pm 0.1K$). The sample pressure was determined by the ruby fluorescence technique, to this
9 purpose a small ruby chip was loaded in the cell together with the sample. For the room
10 pressure measurements, we used water provided by Angelini company (see ref.¹⁴), sealed in
11 a cylindrical glass vial (see section S.1.1 of SI).

21 We measured the water dynamics along two isotherms: at $T = 297 K$ the pressure varies
22 from $0.1 MPa$ to $750 MPa$, at $T = 273 K$ from 0.1 to $1350 MPa$. The HD-OKE signal,
23 measured at two different pressures and temperatures, is reported in Figure 1. The data
24 show the inter-molecular vibrational dynamics, extending up to about 1 ps, merging into
25 the structural relaxation that lasts longer^{14,33}. The structural relaxation changes with the
26 applied pressure; initially, the relaxation gets faster as pressure increases, while it slows
27 down in consequence of further pressure increments. The effect of pressure on the oscillating
28 part of the signal is less evident in the time-domain data, but it becomes clear in the data
29 transformed to the frequency domain, as it will be shown in the following.

39 The deconvolution process of the time domain HD-OKE signal implies the knowledge of
40 the instrumental function, and requires some assumption on the form of the water response
41 function. The two tasks are of different complexity, depending on the theoretical model used.
42 Data analysis with complex theoretical models, such as those we used to study supercooled
43 water at ambient pressure in the framework of the Mode Coupling Theory (MCT)^{14,32}, re-
44 quires data of very high quality. The method adopted here is definitely less demanding.
45 We assumed (see section S.1.3 of SI) a relatively simple response function, based on a phe-
46 nomenological approach: the slow decay is simulated by the time derivative of a stretched
47 exponential and the vibrational/oscillatory part by the time derivative of two damped har-
48
49
50
51
52
53
54
55
56
57
58
59
60

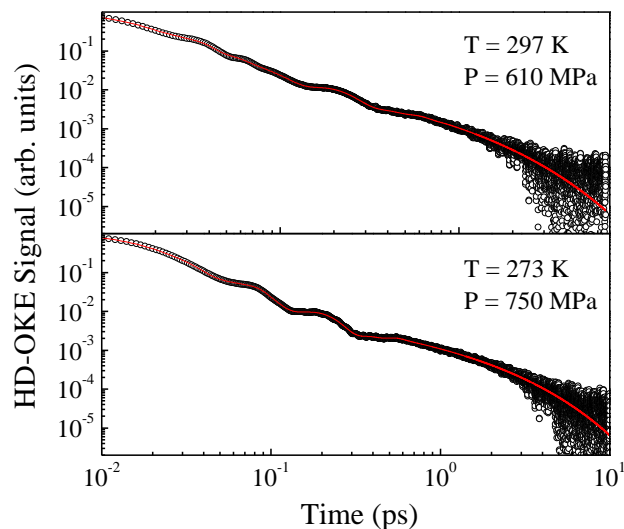


Figure 1: HD-OKE signals measured at two different pressures for the two isotherms. The signal shows, at short times (< 1 ps), fast oscillations due to the inter-molecular vibrational dynamics and, at longer times, the monotonic decay due to structural relaxation.

monic oscillators (see SI, section S.1.3). For what concerns the instrumental function, we build a kind of "artificial" function from the rising profile of the electronic peak of the HD-OKE signal (see SI, section S.1.4). As shown in Fig.1, the used response function fits very well the measured signal in the entire time windows.

The frequency domain response function $\tilde{R}(\omega)$ is obtained as the Fourier transform of the HD-OKE signal $S(t)$. The required deconvolution of the raw data is performed making use of the relation: $Im[\tilde{R}(\omega)] \propto Im\{FT[S(t)]/FT[G(t)]\}$ ^{32,37}, where $G(t)$ is the instrumental function. Two examples of the frequency response function $Im[\tilde{R}(\omega)]$ are reported in Fig.2. These spectra correspond to the low-frequency depolarized Raman signal, corrected for the Bose factor; they consist of two bands, due to intermolecular vibrations. The assignment of the corresponding modes is not obvious; according to a series of computational investigations³⁸⁻⁴¹, the 60 cm^{-1} broad band is dominated by transverse translational motions, corresponding to "bending" of the hydrogen bonds; the 180 cm^{-1} involves motions with essentially longitudinal character, i.e. H-bond "stretching". The slow decay of the OKE signal measured in the time domain corresponds to the very low frequency shoulder that is hardly

visible in the reported spectra.

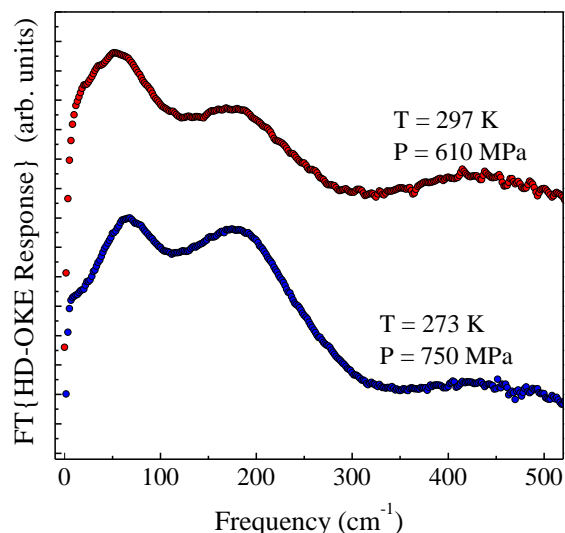


Figure 2: HD-OKE response in the frequency domain, $Im[\tilde{R}(\omega)]$, obtained as the Fourier transform of the time-dependent data shown in Fig.1, after the contribution of the instrumental function has been removed in the deconvolution process.

The slow decay of the signal is fairly well reproduced by the derivative of the stretched exponential. Due to the difficulty of obtaining a reliable value of the stretching exponent, we decide to fix it to the room pressure value of 0.6³³. The mean structural relaxation time (see SI) extracted from the fit was analyzed as a function of pressure. As already reported in the literature for others dynamical properties, namely self-dynamics, self-diffusion constant, rotational correlation time, viscosity^{16-23,25,42,43}, also the structural relation time shows an anomalous trend with increasing pressure. Specifically, it decreases when pressure is applied, reaches a minimum and then increases with the density, following the usual trend of "normal" liquids. The pressure value at the minimum changes with the temperature. This anomalous behavior can be further emphasized by plotting the mean structural times as a function of density, as shown in Fig.3. The density values were computed from the equation of state of water¹. For the two studied isotherms (297 and 273 K), a polynomial fit locates the

¹For the pressure density conversion we used the data of reference⁴⁴. These data cover only the pressure

minimum values of the two curves of Fig.3 at the densities of about 1.095 g/cm^3 and 1.120 g/cm^3 , respectively, corresponding to pressure values of about 285 MPa and 330 MPa .

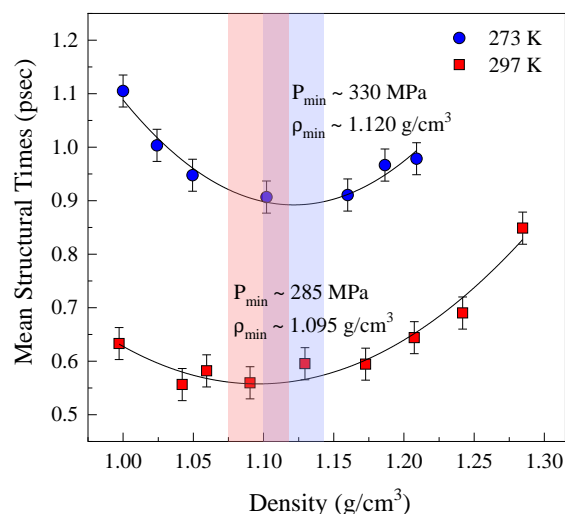


Figure 3: Mean structural relaxation times (see text in Methods) at the densities corresponding to the different applied pressures, obtained from the fit of the slower part of the HD-OKE data with a stretched exponential, for the two isotherms. The structural relaxation time shows an anomalous trend with the density: it decreases applying pressure, reaches a minimum (at a density value that increases with decreasing temperature), and then increases again. Light red and light blue shadowed bands represent the density (pressure) ranges where the minimum can be positioned at the higher and lower temperatures, respectively.

Similar crossover points can be found in the fitting parameters of the oscillating part of the HD-OKE signal. This part, as stated above, is fairly well reproduced by two damped harmonic oscillators (DHOs), corresponding to the two low frequency bands shown in the spectra of Fig.2 around 60 and 180 cm^{-1} . The density dependence of the bending and stretching frequencies (frequency Ω_n of the DHO, see SI, section S.1.3) for the two isotherms 297 and 273 K is shown in Fig.4 and Fig.5, respectively. For the 297 K isotherm, in both bands we can identify two linear regimes with different slopes. The values of the density at which the slope changes occurs are around $\rho = 1.100 \text{ g/cm}^3$ for the stretching band and $\rho = 1.090 \text{ g/cm}^3$ for the bending, values that correspond to pressures of about 295 MPa and range of the stable liquid phase. Our higher pressure values (620 and 750 MPa at at 273 K and 1020 and 1350 MPa at 297 K) fall in the supercooled phase region; we obtain the density values at those pressures by extrapolation from the values in the stable phase.

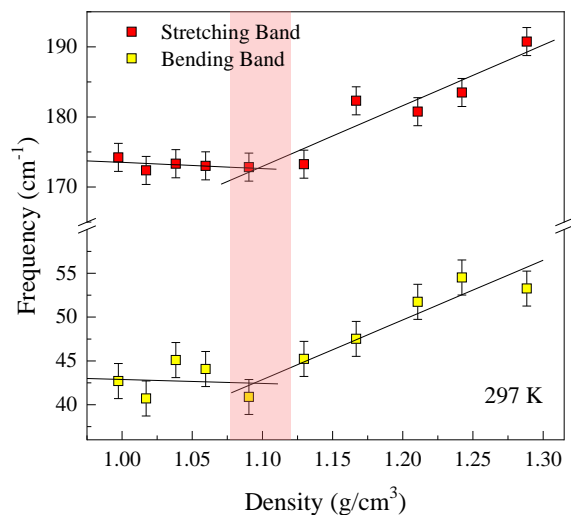


Figure 4: Frequency of bending and stretching peaks at variable densities extracted from the analysis of the HD-OKE signal at 297 K based on two DHOs. Both frequencies show two linear regimes with different slopes; the crossover points are close to that of the structural time in Fig.3. The shadowed band represent the density range where the crossover point can be located, based on data errors.

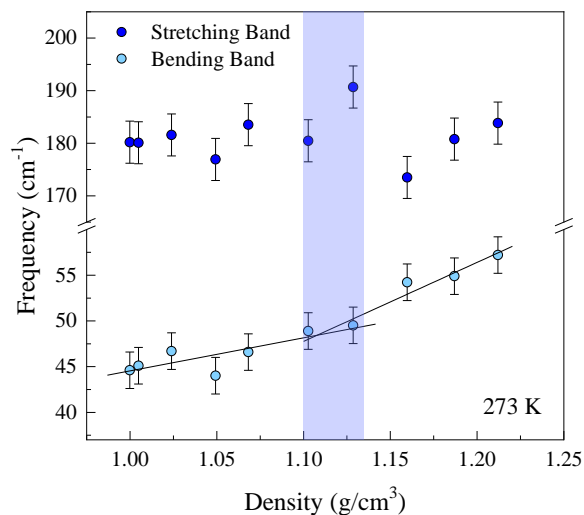


Figure 5: Frequency of bending and stretching peaks at variable densities extracted from the analysis of the HD-OKE signal at 273 K based on two DHOs. The frequency of the bending band shows two linear regimes with different slopes, with a crossover points close to that of the structural time in Fig.3. No well-defined trend can be identified for the stretching frequency. The shadowed band represents the density range where the crossover point can be located, based on data errors.

1
2
3 260 MPa. At the lower temperature, 273 K, instead, the crossover is clearly visible only in
4 the bending band. The determination of the frequency of the stretching band at the lower
5 temperature is more critical; this is due to the large overlap of this band with those at higher
6 frequency, namely the librational contributions, leading to a poorly reliable estimation of the
7 stretching band parameters. In summary, our results clearly identify, at both temperatures,
8 a dynamic crossover for the structural relaxation time. The same is true for the bending
9 peak, while for the stretching band, the bimodal behavior is observed only at 297 K.
10
11
12
13
14
15
16

17 The scaling proprieties of the structural relaxation time in liquids have been often eval-
18 uated using the Stokes-Einstein-Debye models; for liquid water those simple models cannot
19 describe correctly the pressure/temperature dependence of the relaxation times^{45,46}. In sec-
20 tion S.2 of SI, we report a short discussion on the application of these models to our data.
21
22
23
24

25 It is interesting to verify if the trend with pressure of our relaxation times can be de-
26 scribed by the two state model^{3,10,25,29,30}. As we mentioned in the introduction, they describe
27 the liquid water as an athermal non-ideal mixture of two states/structures characterized by
28 different entropies and densities: the LDW and the HDW states. A key parameter of the
29 model is $f(T, P)$, the fraction LDW/(HDW+LDW). This two-state model was utilized by
30 Singh et al.²⁵ to describe some dynamic observables of water (viscosity, diffusivity and ro-
31 tational time) and their pressure dependence. In this picture, the dynamic observable is
32 governed by an effective activation energy, which is an average of the activation energies of
33 the LDW and HDW state, weighted by the fractions f and $1 - f$, respectively. Following
34 this approach, the relaxation time can be written as:
35
36
37
38
39
40
41
42
43
44
45

$$\begin{aligned} \tau(T, P) = & \tau_0 \left(\frac{273.15}{T} \right)^{0.5} \times \\ & \exp \left\{ [1 - f(T, P)] \frac{E_{HDW} + \Delta\nu_{HDW}P}{k_B(T - T_0)} \right. \\ & \left. + f(T, P) \frac{E_{LDW}}{k_B T} \right\} \end{aligned} \quad (1)$$

46
47
48
49
50
51
52
53
54
55
56 In eq.1, water dynamics is treated as that of a mixture of a strong liquid, LDW, with a highly
57
58
59
60

1
2
3 tetrahedral hydrogen bond network, and a fragile liquid, HDW, with a more disordered and
4 close packed structure. The LDW structure is only weakly affected by pressure, and its
5 relaxation time follows an Arrhenius law with E_{LDW} activation energy. The relaxation of
6 the HDW liquid follows a Vogel-Tamann-Fulcher law, with a critical temperature T_0 and a
7 pressure dependent activation energy $E_{HDW} + \Delta\nu_{HDW}P$, $\Delta\nu_{HDW}$ being the volume difference
8 between the activated and initial states. For the calculation of the $f(T, P)$ fraction, we used
9 the code reported in the supplemental material of ref.²⁹ (see section S.3 of the SI). We kept
10 the parameter T_0 fixed at 148 K, the value obtained in the analysis reported in²⁵. With this
11 constrain, the free fitting parameters were E_{LDW} , E_{HDW} and $\Delta\nu_{HDW}$. The curves in Fig.6
12 are the best fit prediction of the two state model, obtained with $E_{LDW}/k_B = 1800 \pm 300K$,
13 $E_{HDW}/k_B = 280 \pm 50K$ and $\Delta\nu_{HDW} = 0.75 \pm 0.2 \cdot 10^{-30}m^3$, values of the same order of
14 magnitude as those reported by Singh et al.²⁵ in their calculation of different dynamical
15 properties. The curves reproduce fairly well the pressure dependence of the experimental
16 mean structural relaxation times, the minima of the two curves being located at 270 MPa
17 and 240 MPa for 297 K and 273 K, respectively. Both these values are both 50 MPa lower
18 than those obtained from the data analysis of Fig. 3 and, most important, preserve the same
19 ordering. The pressure/temperature dependence of the present structural relaxation data
20 are in good agreement with the two state model, cast into Eq.1; therefore, we can affirm
21 that these data push the balance forward a bimodal interpretation of liquid water structures,
22 persisting even at room temperature and high pressure conditions.

23
24
25
26
27
28
29
30
31
32
33
34
35
36
37
38
39
40
41
42
43 It is worth comparing our results with other data present in the literature. In the
44 temperature-pressure phase diagram of water of Fig.7 we report the loci for the extrema of
45 several dynamical properties found in literature^{22,23,25,36} together with our crossover points.
46 All data points are located close to the area where simulations predict the structural trans-
47 ition between the two water forms and the pressure induced collapse of the second shell on
48 the first one. In the same phase diagram, we report the extrema of isothermal compressibil-
49 ity and specific heat calculated from the simulations⁴⁷, and the maximum of the isothermal
50
51
52
53
54
55
56
57
58
59
60

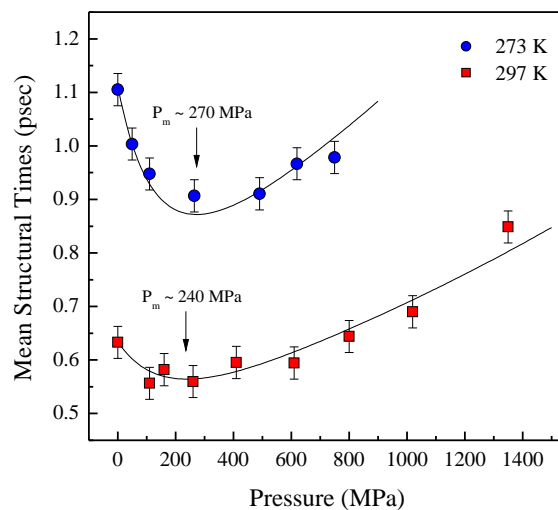


Figure 6: Structural relaxation times (scatter point) as a function of pressure for the two isotherms compared with theoretical values calculated according to the two state model (continuous lines).

compressibility measured at room pressure¹¹. These data points are in the vicinity of the Widom line^{11,48}, which is the continuation of the liquid-liquid phase transition line and emanates from the LLCP in the supercritical region. On the same Widom line, a few studies place the strong-to-fragile dynamics crossover⁴⁹, yet on the same line is the critical temperature T_C of MCT obtained from our OKE data on supercooled water¹⁴ (red star in Fig.7). Within the LLCP scenario, the Widom line and dynamical crossover points possibly identify two critical areas that could be both related to the liquid-liquid critical point. Computer simulation studies on liquids with tetrahedral symmetry⁵⁰ found that two Widom lines can arise from the same LLCP, one with positive slope in the $P - T$ thermodynamic plane and another one with negative slope. On the other hand, another molecular-dynamics simulation study on high pressure water⁵¹ attributes the dynamical crossover to the LD-HD conversion, the latter being just the structural precursor of the high density ice(s). Therefore, in this scenario the line would head towards some high density ice phase transition line and would be unrelated to the hypothetical LLCP.

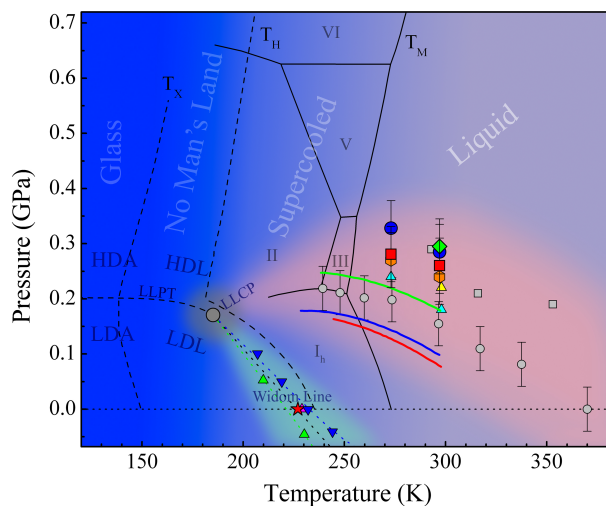


Figure 7: Schematic temperature-pressure phase diagram of water; T_M melting line, T_H homogeneous nucleation line, T_X amorphous ice crystallization line. The HD-OKE investigation in ref.¹⁴ individuates the critical point at atmospheric pressure (red star); the HD-OKE measurements along the two isotherms define the dynamic crossover points: thermodynamic points of the minimum of structural relaxation time (blue circles), slope change values of the frequency of the bending band (red squares), the frequency of the stretching band (green diamond), the minimum of structural relaxation time extracted from the two state model (orange hexagons). Moreover, extrema of the following dynamical properties are shown: slope change of the rotational anisotropy time constant (yellow triangle)²², slope change of the OD stretching vibrational life time (cyan triangles)²², the slope change of the water stretching band as measured by FTIR (grey circles)²³, sound velocity from Brillouin scattering (grey squares)³⁶, self diffusion coefficient (blue line)²⁵, rotational correlation time (green line)²⁵, and viscosity (red line)²⁵. Finally, extrema of isothermal compressibility (blue triangles) and specific heat (green triangles) calculated from the simulations⁴⁷ experimental value of the maximum of isothermal compressibility at room pressure (magenta triangle)¹¹ are shown. The ensemble of data points of different origin identify two regions: the narrow greenish area coincides with the Widom line emanating from the LLCP; the much broader reddish area contains the crossover lines measured for different observables.

1
2
3 In summary, our findings concerning both structural relaxation dynamics and vibrational
4 dynamics, evidently confirm the presence of a dynamical crossover to be related to the struc-
5 tural change of water at different pressures and temperature conditions. The interpretations
6 of these crossover phenomena for the structural relaxation and viscosity observables are in
7 fair agreement with the two state model, showing these crossovers could be in fact the em-
8 anation of LLCP point at high temperature/pressure. In this framework, the bimodal model
9 of water would only be the extension of the LL model at the non-critical thermodynamic
10 conditions, where the HD and LD water phases become local transient fluctuations of the net-
11 work structure. Nevertheless, other experimental investigations are required to definitively
12 determine the proper model for liquid water. In this respect, the feasibility, demonstrated
13 in the present work, of accurate time resolved OKE experiments on pressurized water in
14 anvil cells opens interesting perspective for the experimental study of collective dynamical
15 properties of aqueous samples.
16
17
18
19
20
21
22
23
24
25
26
27
28
29
30

31 **Acknowledgement**

32
33
34 This research was funded by Ente Cassa di Risparmio - Firenze (2016-0866), Ministero
35 dell'Istruzione dell'Università e della Ricerca - Italia (PRIN2017-2017Z55KCW) and European
36 Community by Laserlab-Europe (H2020 EC-GA-654148). We acknowledge M. De Pas, A.
37 Montori and M. Giuntini for providing their continuous assistance in the set-up of the elec-
38 tronics. R. Ballerini and A. Hajeb for the accurate mechanical realizations.
39
40
41
42
43
44
45
46

47 **Supporting Information Available**

48
49
50 A detailed description of the sample preparation, the DAC cell, the experimental technique,
51 and the data analysis is reported in the Supplementary Information file.
52
53
54
55
56
57
58
59
60

References

- (1) Debenedetti, P. Supercooled and Glassy Water. *J. Phys.: Cond. Matt.* **2003**, *15*, R1669–R1726.
- (2) Gallo, P. et al. Water: A Tale of Two Liquids. *Chemical Reviews* **2016**, *116*, 7463–7500.
- (3) Holten, V.; Anisimov, M. A. Entropy-driven liquid-liquid separation in supercooled water. *Scientific reports* **2012**, *2*, 713–713.
- (4) Angell, A. A. Two Phases ? *Nature Materials* **2014**, *13*, 673.
- (5) Soper, A. Continuous Trends. *Nature Materials* **2014**, *13*, 671.
- (6) Debenedetti, P. Debated waters. *Nature Materials* **2014**, *13*, 663.
- (7) Nilsson, A.; Pettersson, L. G. M. The structural origin of anomalous properties of liquid water. *Nature Communications* **2015**, *6*, 8998.
- (8) Russo, J.; Tanaka, H. Understanding water's anomalies with locally favoured structures. *Nat Commun* **2014**, *5*, 3556.
- (9) Poole, P. H.; Sciortino, F.; Essmann, U.; Stanley, H. E. Phase behaviour of metastable water. *Nature* **1992**, *360*, 324–328.
- (10) Huang, C. et al. The inhomogeneous structure of water at ambient conditions. *Proc. Nat. Acad. Sci. USA* **2009**, *102*, 15214–15218.
- (11) Kim, K. H.; Späh, A.; Pathak, H.; Perakis, F.; Mariedahl, D.; Amann-Winkel, K.; Sellberg, J. A.; Lee, J. H.; Kim, S.; Park, J.; Nam, K. H.; Katayama, T.; Nilsson, A. Maxima in the thermodynamic response and correlation functions of deeply supercooled water. *Science* **2017**, *358*, 1589–1593.
- (12) Sellberg, J. A. et al. Ultrafast X-ray probing of water structure below the homogeneous ice nucleation temperature. *Nature* **2014**, *510*, 381–4.

- 1
2
3
4 (13) Pallares, G.; Azouzi, M. E.; Gonzalez, M. A.; Aragoes, J. L.; Abascal, J. L. F.; Valeri-
5 ani, C.; Caupin, F. Anomalies in bulk supercooled water at negative pressure. *Proceed-*
6 *ings of the National Academy of Sciences of the United States of America* **2014**, *111*,
7 7936–7941.
8
9
10
11
12 (14) Taschin, A.; Bartolini, P.; Eramo, R.; Righini, R.; Torre, R. Evidence of two distinct
13 local structures of water from ambient to supercooled conditions. *Nature Communica-*
14 *tions* **2013**, *4*, 2401.
15
16
17
18 (15) Perakis, F.; Marco, L. D.; Shalit, A.; Tang, F.; Kann, Z. R.; Kuhne, T. D.; Torre, R.;
19 Bonn, M.; Nagata, Y. Vibrational Spectroscopy and Dynamics of Water. *Chem Rev*
20 **2016**, *116*, 7590–7607.
21
22
23
24
25 (16) Prielmeier, F. X.; Lang, E. W.; Speedy, R. J.; Lüdemann, H.-D. The Pressure Depend-
26 ence of Self Diffusion in Supercooled Light and Heavy Water. *Berichte der Bunsen-*
27 *gesellschaft für physikalische Chemie* **1988**, *92*, 1111–1117.
28
29
30
31
32 (17) Harris, K. R.; Newitt, P. J. Self-Diffusion of Water at Low Temperatures and High
33 Pressure. *Journal of Chemical & Engineering Data* **1997**, *42*, 346–348.
34
35
36
37 (18) Kawamoto, T.; Ochiai, S.; Kagi, H. Changes in the structure of water deduced from the
38 pressure dependence of the Raman OH frequency. *J Chem Phys* **2004**, *120*, 5867–70.
39
40
41
42 (19) Cunsolo, A.; Orecchini, A.; Petrillo, C.; Sacchetti, F. Quasielastic neutron scattering
43 investigation of the pressure dependence of molecular motions in liquid water. *J Chem*
44 *Phys* **2006**, *124*, 084503.
45
46
47
48 (20) Goncharov, A.; Goldman, N.; Fried, L.; Crowhurst, J.; Kuo, I. F.; Mundy, C.; Zaug, J.
49 Dynamic Ionization of Water under Extreme Conditions. *Physical Review Letters* **2005**,
50 *94*, 125508–125508.
51
52
53
54
55
56
57
58
59
60

- 1
2
3 (21) Bove, L. E.; Klotz, S.; Strassle, T.; Koza, M.; Teixeira, J.; Saitta, A. M. Translational
4 and rotational diffusion in water in the Gigapascal range. *Phys Rev Lett* **2013**, *111*,
5 185901.
6
7
8
9
10 (22) Fanetti, S.; Lapini, A.; Pagliai, M.; Citroni, M.; Di Donato, M.; Scandolo, S.;
11 Righini, R.; Bini, R. Structure and dynamics of low-density and high-density liquid
12 water at high pressure. *J. Phys. Chem. Letters* **2014**, *5*, 235–240.
13
14
15
16 (23) Fanetti, S.; Pagliai, M.; Citroni, M.; Lapini, A.; Scandolo, S.; Righini, R.; Bini, R. Con-
17 necting the Water Phase Diagram to the Metastable Domain: High-Pressure Studies
18 in the Supercooled Regime. *J. of Phys. Chem. Lett.* **2014**, *5*, 3804–3809.
19
20
21
22
23 (24) Lapini, A.; Pagliai, M.; Fanetti, S.; Citroni, M.; Scandolo, S.; Bini, R.; Righini, R.
24 Pressure Dependence of Hydrogen-Bond Dynamics in Liquid Water Probed by Ultrafast
25 Infrared Spectroscopy. *The Journal of Physical Chemistry Letters* **2016**, *7*, 3579–3584,
26 PMID: 27560355.
27
28
29
30
31 (25) Singh, L. P.; Issenmann, B.; Caupin, F. Pressure dependence of viscosity in supercooled
32 water and a unified approach for thermodynamic and dynamic anomalies of water.
33 *Proceedings of the National Academy of Sciences* **2017**, *114*, 4312–4317.
34
35
36
37
38 (26) Vedamuthu, M.; Singh, S.; Robinson, G. W. Properties of Liquid Water: Origin of the
39 Density Anomalies. *The Journal of Physical Chemistry* **1994**, *98*, 2222–2230.
40
41
42
43 (27) Tanaka, H. Simple physical model of liquid water. *The Journal of Chemical Physics*
44 **2000**, *112*, 799–809.
45
46
47
48 (28) Tanaka, H. A new scenario of the apparent fragile-to-strong transition in tetrahedral
49 liquids: water as an example. *Journal of Physics: Condensed Matter* **2003**, *15*, L703–
50 L711.
51
52
53
54
55
56
57
58
59
60

- 1
2
3 (29) Holten, V.; Sengers, J. V.; Anisimov, M. A. Equation of State for Supercooled Water
4 at Pressures up to 400 MPa. *Journal of Physical and Chemical Reference Data* **2014**,
5 *43*, 043101.
6
7
8
9
10 (30) Holten, V.; Palmer, J. C.; Poole, P. H.; Debenedetti, P. G.; Anisimov, M. a. Two-state
11 thermodynamics of the ST2 model for supercooled water. *The Journal of chemical*
12 *physics* **2014**, *140*, 104502–104502.
13
14
15
16 (31) Shi, R.; Russo, J.; Tanaka, H. Origin of the emergent fragile-to-strong transition in
17 supercooled water. *Proceedings of the National Academy of Sciences* **2018**, *115*, 9444–
18 9449.
19
20
21
22
23 (32) Taschin, A.; Bartolini, P.; Eramo, R.; Righini, R.; Torre, R. Optical Kerr effect of liquid
24 and supercooled water: The experimental and data analysis perspective. *J. Chem. Phys.*
25 **2014**, *141*, 084507.
26
27
28
29
30 (33) Torre, R.; Bartolini, P.; Righini, R. Structural relaxation in super-cooled water by
31 time-resolved spectroscopy. *Nature* **2004**, *428*, 296–298.
32
33
34
35 (34) Ishizumi, A.; Kasami, M.; Mishina, T.; Yamamoto, S.; Nakahara, J. Optical Kerr Effect
36 in Carbon Disulfide under High Pressure. *High Pressure Research* **2003**, *23*, 201–204.
37
38
39
40 (35) Krisch, M.; Loubeyre, P.; Ruocco, G.; Sette, F.; Cunsolo, A.; Astuto, M. D.; Letoul-
41 lec, R.; Lorenzen, M.; Mermet, A.; Verbeni, R.; D'SAstuto, M.; Monaco, G. Pressure
42 Evolution of the High-Frequency Sound Velocity in Liquid Water. *Physical Review Let-*
43 *ters* **2002**, *89*, 125502–125502.
44
45
46
47
48 (36) Li, F.; Cui, Q.; He, Z.; Cui, T.; Zhang, J.; Zhou, Q.; Zou, G.; Sasaki, S. High pressure-
49 temperature Brillouin study of liquid water: evidence of the structural transition from
50 low-density water to high-density water. *J Chem Phys* **2005**, *123*, 174511.
51
52
53
54
55
56
57
58
59
60

- 1
2
3 (37) P.Bartolini,; Taschin, A.; Eramo, R.; Torre, R. Optical Kerr Effect Experiments on
4 Complex Liquids, A Direct Access to Fast Dynamic Processes. Time-Resolved Spectro-
5 scopy in Complex Liquids. New York, 2008; pp 73–127.
6
7
8
9
10 (38) Skaf, M.; Sonoda, M. Optical Kerr effect in supercooled water. *Phys. Rev. Lett.* **2005**,
11 *94*, 137802.
12
13
14 (39) DeSantis, A.; Ercoli, A.; Rocca, D. Comment on "An interpretation of the low-
15 frequency spectrum of liquid water" J. Chem. Phys. 118, 452 (2003). *J. Chem. Phys.*
16 **2004**, *120*, 1657–1658.
17
18
19
20
21 (40) Padró, J. A.; Martí, J. Response to "Comment on "An interpretation of the low-
22 frequency spectrum of liquid water" J. Chem. Phys. 118, 452 (2003)". *J. Chem.*
23 *Phys.* **2004**, *120*, 1659–1660.
24
25
26
27
28 (41) Ito, H.; Hasegawa, T.; Tanimura, Y. Effects of Intermolecular Charge Transfer in Liquid
29 Water on Raman Spectra. *J Phys Chem Lett* **2016**, 4147–4151.
30
31
32
33 (42) Lang, E. W.; Lüdemann, H. D. High Pressure O-17 Longitudinal Relaxation Time
34 Studies in Supercooled H₂O and D₂O. *Berichte der Bunsengesellschaft für physikalische*
35 *Chemie* **1981**, *85*, 603–611.
36
37
38
39
40 (43) Arnold, M. R.; Lüdemann, H.-D. The pressure dependence of self-diffusion and
41 spin-lattice relaxation in cold and supercooled H₂O and D₂O. *Phys. Chem. Chem.*
42 *Phys.* **2002**, *4*, 1581–1586.
43
44
45
46
47 (44) Wagner, W.; PruSS, A. The IAPWS Formulation 1995 for the Thermodynamic Prop-
48 erties of Ordinary Water Substance for General and Scientific Use. *Journal of Physical*
49 *and Chemical Reference Data* **2002**, *31*, 387–535.
50
51
52
53
54 (45) Mazza, M. G.; Giovambattista, N.; Stanley, H. E.; Starr, F. W. Connection of trans-
55
56
57
58
59
60

- 1
2
3 lational and rotational dynamical heterogeneities with the breakdown of the Stokes-
4 Einstein and Stokes-Einstein-Debye relations in water. *Phys. Rev. E* **2007**, *76*, 031203.
5
6
7
8 (46) Kumar, P. Breakdown of the Stokes–Einstein relation in supercooled water. *Proceedings*
9 *of the National Academy of Sciences* **2006**, *103*, 12955–12956.
10
11
12 (47) González, M. A.; Valeriani, C.; Caupin, F.; Abascal, J. L. F. A comprehensive scenario
13 of the thermodynamic anomalies of water using the TIP4P/2005 model. *The Journal*
14 *of Chemical Physics* **2016**, *145*, 054505.
15
16
17 (48) Kumar, P.; Franzese, G.; Stanley, H. E. Predictions of Dynamic Behavior under Pressure
18 for Two Scenarios to Explain Water Anomalies. *Physical Review Letters* **2008**, *100*.
19
20
21 (49) De Marzio, M.; Camisasca, G.; Rovere, M.; Gallo, P. Fragile to strong crossover and
22 Widom line in supercooled water: A comparative study. *Frontiers of Physics* **2017**, *13*,
23 136103.
24
25
26 (50) Buldyrev, S. V.; Franzese, G. Two types of dynamic crossovers in a network-forming
27 liquid with tetrahedral symmetry. *Journal of Non-Crystalline Solids* **2015**, *407*, 392–
28 398.
29
30
31 (51) Saitta, A. M.; Datchi, F. Structure and phase diagram of high-density water: The role
32 of interstitial molecules. *Phys. Rev. E* **2003**, *67*, 020201.
33
34
35
36
37
38
39
40
41
42
43
44
45
46
47
48
49
50
51
52
53
54
55
56
57
58
59
60

Graphical TOC Entry

